

Effect of MnO₂ on the dielectric and piezoelectric properties of Alkaline Niobate based lead free piezoelectric ceramics.

Henry Ekene Mgbemere, Ralf-Peter Herber and Gerold A. Schneider

Institute of Advanced Ceramics, Hamburg University of Technology, Germany
Denickestrasse 15, 21073, Hamburg.

Corresponding author. email: g.schneider@tu-harburg.de
[doi:10.1016/j.jeurceramsoc.2008.10.012](https://doi.org/10.1016/j.jeurceramsoc.2008.10.012)

Abstract

Lead free ferroelectric ceramics of the KNN–LiTaO₃–LiSbO₃ system were prepared using the mixed oxide route. This work reports the effect of doping (K_{0.44}Na_{0.52}Li_{0.04})(Nb_{0.86}Ta_{0.1}Sb_{0.04})O₃ produced through the conventional solid state sintering method with different amounts of MnO₂. With 1 mol% of the dopant, ~ 96.5% of the theoretical density of the ceramics was achieved while grain growth inhibition was attained through pinning of the grain boundary movement. A polymorphic phase transition (PPT) was induced in the ceramic from the orthorhombic crystal structure to the tetragonal structure with increasing dopant amount. At lower temperatures, the doped samples had higher epsilon values but there was a decrease in both *T_c* (from 333 °C to 249 °C) and epsilon value at *T_c* (from ≈9500 to <6000). At temperatures below 300 °C however, the loss tangent in the doped samples (≈2.5 mol%) was much lower and steady when compared to the undoped one. The ferroelectric properties were slightly lowered with the addition of MnO₂. The remnant polarisation (*P_r*) was lowered from ~18μC/cm² to ~9μC/cm², the coercive field (*E_c*) from ~ 8.5 kV/cm to ~ 6.2 kV/cm and the piezoelectric charge coefficient (*d₃₃*) decreased as well.

Keywords: Dielectric properties; Ferroelectric properties; Piezoelectric properties; Perovskites; Lead free

I. Introduction

Lead zirconate titanate (PZT) based piezo-ceramics have been widely used in the manufacture of actuators, sensors, transducers and in other electromechanical devices because of their excellent piezoelectric properties. However lead in most cases constitutes more than 60 % of the composition of these piezo-ceramics. Lead as a material is highly toxic and because of its volatility and high vapour pressure, is released to the atmosphere during sintering causing serious environmental and health problems. Another cause for concern is its disposal at the end of the life cycle of these products. Considering all these health concerns posed by lead, multinational governments like the European Union have enacted laws that ban the use of lead in the manufacture of many products¹. In the field of electro-ceramics, concessions were allowed considering the fact that many of the lead free ferroelectric ceramics have piezoelectric properties that are very inferior when compared to those of lead based piezoceramics. There is a need to replace lead in the field of piezoelectric ceramics.

A lot of research has been carried out on lead free piezoceramics in the last fifty years but in the last five years, the momentum has tremendously increased accounting for about 75% of all published works. Some of these include KNbO_3 ², $(\text{Ba,Sr})\text{TiO}_3$ (BST), $\text{Bi}_{0.5}\text{K}_{0.5}\text{TiO}_3$ ³ (BKT), $(\text{Bi}_{0.5}\text{Na}_{0.5})\text{TiO}_3$ ⁴ (BNT) and $(\text{K,Na})\text{NbO}_3$ ⁵ based ceramics. Among these materials, $\text{K}_x\text{Na}_{1-x}\text{NbO}_3$ (KNN) which is a solid solution of ferroelectric KNbO_3 and antiferroelectric NaNbO_3 appears to be the most promising because of its comparably high piezoelectric properties, large electromechanical coupling coefficients and high Curie temperature ($\approx 420\text{ }^\circ\text{C}$)⁶. However the sinterability of this product has been difficult without the use of special techniques like hot pressing because of the high volatility of the alkaline element components at high temperature. There is a degradation of the properties ($d_{33} = 80\text{ pC/N}$, $K_p = 0.36$, $\rho = 4.25\text{ g/cm}^3$)⁵ when they are sintered in air whereas hot pressing leads to better properties ($d_{33} = 160\text{ pC/N}$, $K_p = 0.45$, $\rho = 4.46\text{ g/cm}^3$)⁶.

To improve the sinterability and piezoelectric properties of KNN ceramics, a lot of different materials have been used to either dope it or to substitute the main elements. Some of these combinations include: KNN-Ba ⁷, KNN-SrTiO_3 ^{8,9}, KNN-LiNbO_3 ¹⁰, KNN-LiTaO_3 ¹¹, KNN-LiSbO_3 ¹², $(\text{K,Na,Li})(\text{Nb,Ta,Sb})\text{O}_3$ ¹³ and pure KNN with sintering aids like CuO ¹⁴, ZnO ¹⁵, MnO_2 ¹⁶ and Bi_2O_3 ¹⁷. The $\text{KNN-LiTaO}_3\text{-LiSbO}_3$ composition which was reported by Saito et al¹³ remains one of the best so far in terms of piezoelectric properties. This was initially

attributed to the existence of a morphotropic phase boundary (MPB) at the proposed composition. Later reports show however that the addition of dopants lowers the tetragonal to orthorhombic phase transition in the KNN system to room temperature and is therefore rather considered as a polymorphic phase transition (PPT)¹⁸⁻²⁰. Efforts are still being made to see if and how the system can be further improved.

In this work we study the effect of adding MnO₂ on the densification, piezoelectric and dielectric properties of the KNN-LiTaO₃-LiSbO₃ system. Manganese was used because it has been reported to improve the densification of pure KNN¹⁶. Furthermore it is reported to suppress grain growth and helps to increase the electrical resistivity of the piezoceramic.

II. Experimental

The ceramics were synthesized through the mixed oxide route using the following powders; K₂CO₃ (99%), Na₂CO₃ (99%), Li₂CO₃ (99%), Sb₂O₃ (99.9%), Nb₂O₅ (99.9%), Ta₂O₅ (99%) (Chempur Feinchemikalien und Forschungs GmbH, Karlsruhe, Germany.) and MnO₂ (99%) (Alfa Aesar, Karlsruhe, Germany). Stoichiometric compositions of the powders were first weighed and dried at 220 °C for 4h. They were then mixed and attrition milled for four hours using ethanol as solvent and zirconia balls as the milling media. Calcination was carried out at 750 °C for 4 hours after which the same attrition mill and calcination process was repeated.

The powders were pressed into discs of 12.5 mm diameter first using a uni-axial press and later using a cold isostatic press at 200 bars for 2 min. The pellets were sintered in air atmosphere at 1075 °C for 1h. The density of the samples was determined using the Archimedes method while pattern: 00-032-022 from ICDD was used as a reference structure to calculate the theoretical density. The crystalline structure of the sintered samples was examined using X-ray diffraction analysis with CuK α radiation (D8 Discover, Bruker AXS, Karlsruhe, Germany). The samples were polished and thermally etched at 925 °C for 30 min. The microstructure was observed using a scanning electron microscope (LEO 1530 FESEM, Gemini/Zeiss, Oberkochen, Germany). Grain size measurements were carried out using the mean intercept length method from at least six different areas of the SEM image. Silver paint acting as electrodes was applied on both surfaces of the sample. The temperature dependence of the dielectric properties of the ceramics was measured from 20 Hz to 1 MHz using an LCR meter (HP 4284A, Agilent Technologies, Inc., Palo Alto, USA) attached to a programmable furnace. The polarisation hysteresis curves were obtained using a Sawyer-Tower circuit while unipolar and dipolar strain hysteresis curves were obtained using an inductive transducer

device. A complete hysteresis loop was performed in 3 min. The piezoelectric coefficient (d_{33}) was measured using a low signal displacement transducer connected to a lock-in amplifier which measures the amplitude.

III. Result and discussion

The density values for the KNN–LiTaO₃–LiSbO₃ ceramics doped with MnO₂ are as shown in Table 1. The theoretical density for the undoped sample is 4.79 g/cm₃ while the relative density was calculated to be 94.3%. Densification is improved up to 96.4% when an amount of 1 mol% MnO₂ is added. This is accompanied by a decrease in grain growth which is in agreement with other reports for pure KNN.^{22,23} The SEM images of the thermally etched samples in both the undoped and doped form are shown in Fig. 1. For both compositions, cornered cubic grains were observed in the surfaces of the polished samples. The microstructures of the samples have some smooth and rough grains. This may be due to the different crystallographic planes, which behave differently during thermal etching. The higher energetic planes try to revert to the lower energetic planes and the result is a steeped/rough surface. For the undoped sample (Fig. 1a), there is an inhomogeneous grain size distribution such that the grains have a bimodal grain size distribution with big grains being surrounded by small grains. The calculated average grain sizes are $7.3\pm 0.1\mu\text{m}$ and $2.1\pm 0.1\mu\text{m}$ for the big and small grains, respectively. Unevenly distributed relatively large pores can be seen at the grain boundaries.

The shapes of the pores show that some of them may have been formed due to grain pull-out during polishing process than due to sintering. In Fig. 1b, the sample doped with 0.5 mol% of MnO₂ shows a unimodal grain size distribution with an average grain size of approximately $2.1\pm 0.1\mu\text{m}$ showing that the grain growth anomaly in the undoped sample is suppressed here because manganese is known to create oxygen vacancies thereby pinning the movement of the grain boundaries. Some researchers^{24,25} have attributed this to the fact that Mn ions occupy both the A and B sites of the perovskite structure. It is said that when PZT is doped with MnO₂, the site occupancy is determined by the amount of the dopant in the ceramic. Below 0.5 mol%, MnO₂ is believed to act as a donor and above that as an acceptor by occupying A-sites and B-sites, respectively. It is believed that this behaviour extends to the KNN solid solution.²³

The XRD pattern of polished samples doped with different amounts of MnO_2 is shown in Fig. 2a. All the ceramics have a perovskite structure and in the undoped sample, the orthorhombic structure is the dominant phase at room temperature and changes to a predominantly tetragonal structure with increasing the amount of the dopant showing that the tetragonal-orthorhombic phase transition ($T_{\text{T-O}}$) is shifted to lower temperatures with addition of MnO_2 . Fig. 2b shows the change in the structure at 2θ angle of between 45° and 47° with increasing amount of MnO_2 . The contribution of the different peak shapes to orthorhombic and tetragonal structures was shown by Wang and Li.²⁶ Extra peaks (marked with a square) that appear with increasing amounts of the additive show that the solubility of MnO_2 in the $\text{KNN-LiTaO}_3\text{-LiSbO}_3$ solid solution is limited. The excess is believed to accumulate at the grain boundaries.²² Peak search and match analysis was carried out using the ICDD, but due to their size these extra peaks could not be conclusively attributed to any structure.²⁷ Fig. 3a shows the temperature dependent values of dielectric constant while Fig. 3b shows the loss tangent for the MnO_2 doped samples measured at 1 kHz. The addition of the Li^+ , Ta^{5+} and Sb^{5+} to pure KNN leads to the formation of a PPT reducing the first order phase transition to around room temperature.²⁶

The $\text{KNN-LiTaO}_3\text{-LiSbO}_3$ system exhibits two phase transition peaks: The first is associated with $T_{\text{T-O}}$ near room temperature while the second is with the tetragonal to cubic phase transition at 333°C and a dielectric peak of approximately 9500. These values are high when compared to the results by other researchers¹³. This could be a result of the difference in the sintering atmosphere used, powder processing methods and parameters used or even from the starting raw materials. Addition of MnO_2 reduces the T_c to about 249°C which did not decrease much further with increased doping amount. Addition of dopants is known to change microstructures substantially and affect crystalline phase of samples¹⁸. The doped samples have rounded peaks which is an indication of a decrease in ferroelectricity. The dielectric loss values in Fig. 3b show that the addition of the dopants reduced the dielectric loss in the samples to approximately 2.5% at temperatures below 300°C . The loss in the undoped sample is however higher than those obtained by other researchers.^{18,28} For the manufacturing of devices like transformers that require very low dielectric loss values even at elevated temperatures, the doped composition could be explored as has been done in some reports.²⁹

The polarisation hysteresis curves for the undoped and doped samples are shown in Fig. 4. The entire curves show saturation polarisation when an electric field ~ 20 kV/cm is applied.

The addition of manganese lowered the coercive field (E_c) and the remnant polarisation values. This is interesting because lower coercive fields are usually attributed to donor doped piezoceramics while lower remnant polarisations are commonly found in acceptor doped ceramics. Additionally the doped ceramics exhibit a lower area of the hysteresis loop and as a result hysteretic losses are lower too. However, there is no significant difference with increasing amount of dopant. In Fig. 5, the strain hysteresis loops of the undoped and manganese doped ceramics are shown. All compositions had the typical butterfly shape which shows that they are ferroelectric. The doped ceramics all exhibited a smaller hysteretic behaviour than the undoped ceramic. This may be explained by the acceptor doping effect of the dopant on KNN–LiTaO₃–LiSbO₃ ceramics. The highest value of the piezoelectric charge coefficient (d_{33}) for the samples as shown in Table 1 is from the undoped sample. The amount of MnO₂ added did not significantly change the d_{33} values. The reason for the reduction could be attributed to the fact that addition of the dopants led to a decrease in the distortion of the crystal structure as can be seen in the reduced peak splitting in Fig. 2.

IV. Conclusion

Addition of MnO₂ to the KNN–LiTaO₃–LiSbO₃ improved the density of the sintered ceramics by inhibiting grain growth. The addition of MnO₂ induced a phase transformation from orthorhombic to the tetragonal structure at room temperature, a decrease in the T_c and a slight shift in the T_{T-O} phase transition. The dielectric loss values were reduced by doping with MnO₂ even at higher temperatures. Adding MnO₂ led to a reduction in the piezoelectric charge coefficient (d_{33}), the remanent polarisation, coercive field and strain hysteresis loops, respectively. Increasing amounts of dopants result in the formation of extra phases and do not significantly change the piezoelectric properties.

Acknowledgements

This work was supported by the scholarship granted by the European commission through the Erasmus Mundus programme for masters' degree studies in materials science.

References

1. Council Epat, Directive 2002/95/EC of the European parliament and of the council of January 2003 on the restriction of the use of hazardous substances in electrical and electronic equipment. *Eur. J.*, 2003, **37**, 19.
2. Toda, K., Ohtake, N., Kawakami, M., Tokuoka, S., Uematsu, K. and Sato,

- M., Characterisation of potassium niobate produced by self-assembled nanosheet from aqueous solution. *Jpn. J. Appl. Phys.*, 2002, **41**(11B), 7021–7024.
3. Hiruma, Y., Aoyagi, R., Nagata, H. and Takenaka, T., Ferroelectric and piezoelectric properties of $(\text{B}_{1/2}\text{K}_{1/2})\text{TiO}_3$ ceramics. *Jpn. J. Appl. Phys.*, 2005, **44**(7A), 5040–5044.
4. Takenaka, T., Sakata, K. and Toda, K., Piezoelectric properties of $(\text{Bi}_{1/2}\text{Na}_{1/2})\text{TiO}_3$ -based ceramics. *Ferroelectrics*, 1990, **106**, 375–380.
5. Egerton, L. and Dillion, D. M., Piezoelectric and dielectric properties of ceramics in the system potassium–sodium niobate. *J. Am. Ceram. Soc.*, 1959, **42**, 438–442.
6. Jaeger, R. E. and Egerton, L., Hot pressing of potassium–sodium niobates. *J. Am. Ceram. Soc.*, 1962, **45**, 209–213.
7. Ahn, Z. S. and Schulze, W. A., Conventionally sintered $(\text{Na}_{0.5}\text{K}_{0.5})\text{NbO}_3$ with barium additions. *J. Am. Ceram. Soc.*, 1987, **70**, 18–21.
8. Guo, Y., Kakimoto K.-i. and Ohsato, H., Dielectric and piezoelectric properties of lead-free $(\text{Na}_{0.5}\text{K}_{0.5})\text{NbO}_3$ - SrTiO_3 ceramics. *Solid State Commun.*, 2004, **129**, 279–284.
9. Kosec, M., Bobnar, V., Hrovat, M., Bernard, J., Malic, B. and Holc, J., New lead-free relaxors based on the $\text{K}_{0.5}\text{Na}_{0.5}\text{NbO}_3$ - SrTiO_3 solid solution. *J. Mater. Res.*, 2004, **19**(6), 1849–1854.
10. Kakimoto K.-i., Akao, K., Guo, Y. and Ohsato, H., Raman scattering study of piezoelectric $(\text{Na}_{0.5}\text{K}_{0.5})\text{NbO}_3$ - LiNbO_3 ceramics. *Jpn. J. Appl. Phys.*, 2005, **44**(9B), 7064–7067.
11. Hollenstein, E., Davis, M., Damjanovic, D. and Setter, N., Piezoelectric properties of Li and Ta modified $(\text{K}_{0.5}\text{Na}_{0.5})\text{NbO}_3$ ceramics. *Appl. Phys. Lett.*, 2005, **87**, 182905, pp. 1–3.
12. Zang, G.-Z., Wang, J.-F., Chen, H.-C., Su, W.-B., Wang, C.-M., Qi, P., Ming, B.-Q., Du, J. and Zheng, L.-M., Perovskite $(\text{Na}_{0.5}\text{K}_{0.5})_{1-x}(\text{LiSb})_x\text{Nb}_{1-x}\text{O}_3$ lead-free piezoceramics. *Appl. Phys. Lett.*, 2006, **88**, 212908, pp. 1–3.
13. Saito, Y., Takao, H., Tani, T., Nonoyama, T., Takatori, K., Homma, T., Nagaya, T. and Nakamura, M., Lead-free piezoceramics. *Nature*, 2004, **432**, 84–87.
14. Matsubara, M. and Kikuta, K. S. H., Piezoelectric properties of $(\text{K}_{0.5}\text{Na}_{0.5})(\text{Nb}_{1-x}\text{Ta}_x)\text{O}_3$ - $\text{K}_{5.4}\text{CuTa}_{10}\text{O}_{29}$ ceramics. *J. Appl. Phys.*, 2005, **97**, 114105, pp. 1–7.
15. Chen, R. and Li, L., Sintering and electrical properties of lead-free $\text{Na}_{0.5}\text{K}_{0.5}\text{NbO}_3$ piezoelectric ceramics. *J. Am. Ceram. Soc.*, 2006, **89**(6), 2010–2015.
16. Ahn, C.-W., Song, H.-C., Nahm, S., Park, S.-H., Uchino, K., Priya, S., Lee, H.-G. and Nam-Kee, K., Effect of MnO_2 on the piezoelectric properties of $(1-x)(\text{Na}_{0.5}\text{K}_{0.5})\text{NbO}_3$ - $x\text{BaTiO}_3$ ceramics. *Jpn. J. Appl. Phys.*, 2005, **44**, L1361–L1364.
17. Du, H., Liu, D., Tang, F., Zhu, D. and Wancheng, Z., Microstructure, piezoelectric, and ferroelectric properties of Bi_2O_3 -added $(\text{K}_{0.5}\text{Na}_{0.5})\text{NbO}_3$ lead-free ceramics. *J. Am. Ceram. Soc.*, 2007, **90**, 2824–2829.
18. Hagh, N. M., Jadidian, B. and Safari, A., Property-processing relationship in lead-free (K, Na, Li) NbO_3 -solid solution system. *J. Electroceram.*, 2007, **18**, 339–346.
19. Shrout, T. R., Eitel, R., Randall, C. A., Alberta, E. and Rehrig, P. W., New high temperature morphotropic phase boundary piezoelectric ceramics, applications of ferroelectrics, ISAF 2002. In *Proceedings of the 13th IEEE International Symposium on ferroelectrics*, 2002, pp. 277–280.
20. Shrout, T. R., Zhang, S. J., Eitel, R., Stringer, C. and Randall, C. A., High performance, high temperature perovskite piezoelectrics, applications of ferroelectrics, ISAF-04. In *14th IEEE International Symposium*, 2004, pp.26–129.
21. Akdogan, E. K., Kerman, K., Abazari, M. and Safari, A., Origin of high piezoelectric activity in ferroelectric $(\text{K}_{0.44}\text{Na}_{0.52}\text{Li}_{0.04})(\text{Nb}_{0.84}\text{Ta}_{0.1}\text{Sb}_{0.06})\text{O}_3$ ceramics. *Appl. Phys. Lett.*, 2008, **92**, 112908, pp.1–3.

22. Tashiro, S., Ishii, K. and Wada, T., Fabrication of $(\text{Sr}_x\text{K}_{0.5-x}\text{Na}_{0.5-x})\text{NbO}_3$ piezoelectric ceramics and effects of MnO addition on their piezoelectric properties. *Jpn. J. Appl. Phys.*, 2006, **45**(9B), 7449–7454.
23. Lin, D., Kwok, K.W., Tian, H., Wong, H. and Chan, L-w., Phase transitions and electrical properties of $(\text{Na}_{1-x}\text{K}_x)(\text{Nb}_{1-y}\text{Sb}_y)\text{O}_3$ lead-free piezoelectric ceramics with a MnO_2 sintering aid. *J. Am. Ceram. Soc.*, 2007, **90**, 1458–1462.
24. He L.-x. and Li, C.-e., Effects of addition of MnO on piezoelectric properties of lead zirconate titanate. *J. Mater. Sci.*, 2000, **35**, 2477–2480.
25. Klimov, V. V., Selikova, N. I. and Bronnikov, A. N., Effect of MnO_2 , Bi_2O_3 , and ZnO additions on the electrical properties of lead zirconate titanate piezoceramics. *Inorg. Mater.*, 2006, **42**(5), 573–577.
26. Wang, K. and Li, J.-F., Analysis of crystallographic evolution in $(\text{Na,K})\text{NbO}_3$ -based lead free piezoelectrics by X-ray diffraction. *Appl. Phys. Lett.*, 2007, **91**, 262902, pp. 1–3.
27. Ming, B.-Q., Wang, J.-F., Qi, P. and Zang, G.-Z., Piezoelectric properties of (Li,Sb,Ta) modified $(\text{Na,K})\text{NbO}_3$ lead-free ceramics. *J. Appl. Phys.*, 2007, **101**, 054103, pp. 1–4.
28. Hagh, N. M., Ashbahian, E. and Safari, A., Lead-free piezoelectric ceramic transducer in the $\text{K}_{1/2}\text{Na}_{1/2}\text{NbO}_3$ -solid solution system. *IEEE-UFFC Trans.*, 2008, **55**(1), 214–224.
29. Guo, M., Lam, K. H., Lin, D. M., Wang, S., Kwok, K.W., Chan, H. L.W. and Zhao, X. Z., A Rosen-type piezoelectric transformer employing lead-free $\text{K}_{0.5}\text{Na}_{0.5}\text{NbO}_3$ ceramics. *J. Mater. Sci.*, 2008, **43**, 709–714.

Figure Captions

Fig. 1

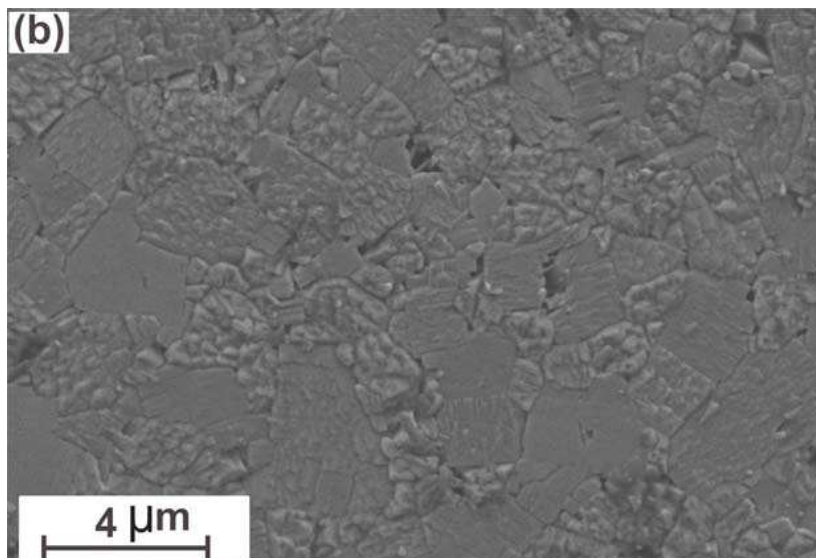
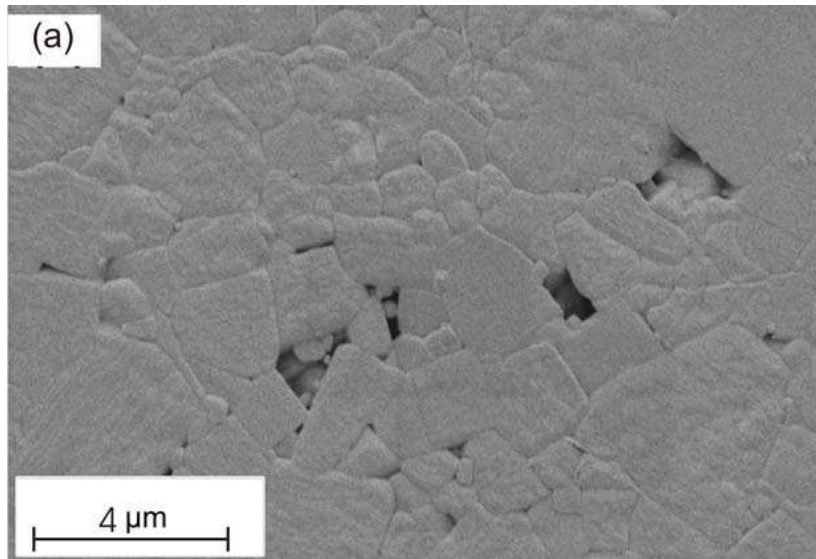


Fig. 1 SEM micrographs of the thermally etched KNN-LiTaO₃-LiSbO₃ samples that were sintered at 1075 °C for 1 hour (a) undoped, (b) 0.5 mol % MnO₂

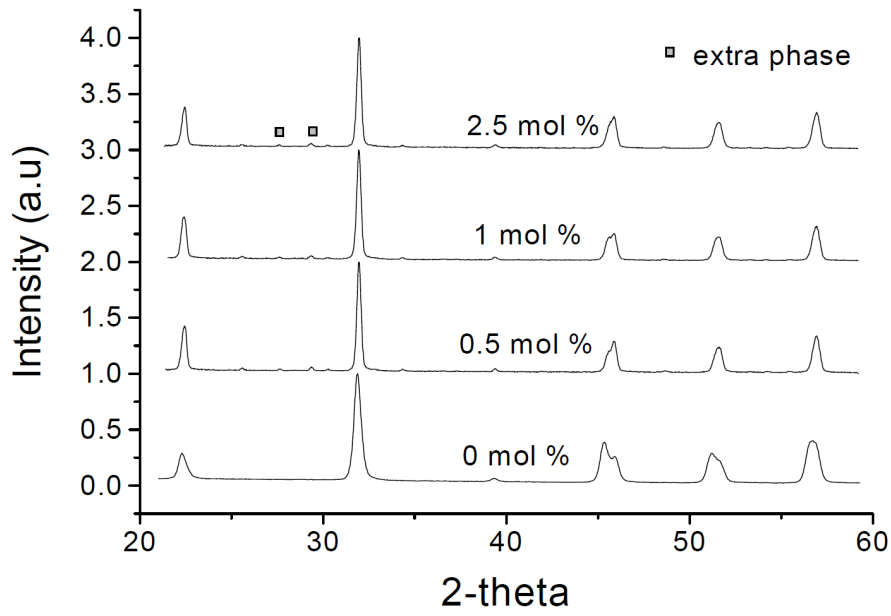


Fig. 2a

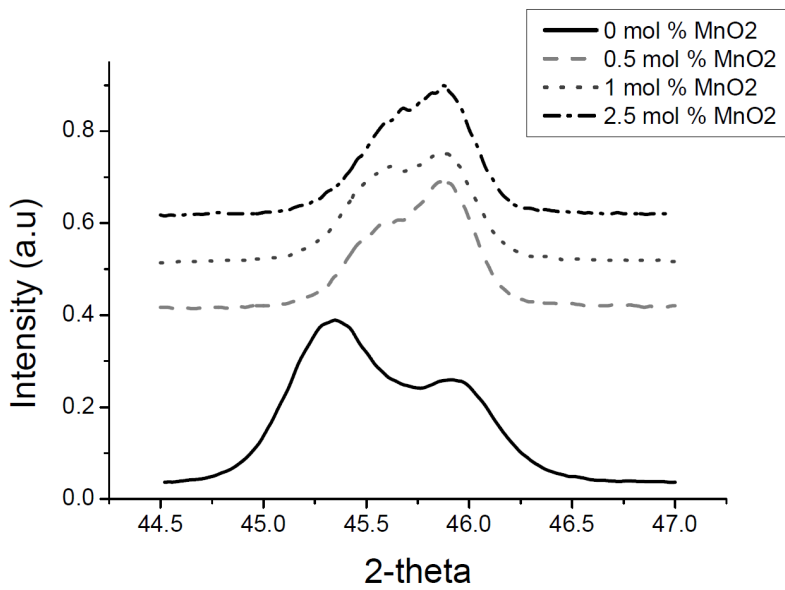


Fig. 2b

Fig. 2 XRD patterns of the KNN-LiTaO₃-LiSbO₃ samples (a) doped with different amounts of MnO₂, (b) zoomed pattern from 44.5° to 47° showing the change from orthorhombic to tetragonal structure.

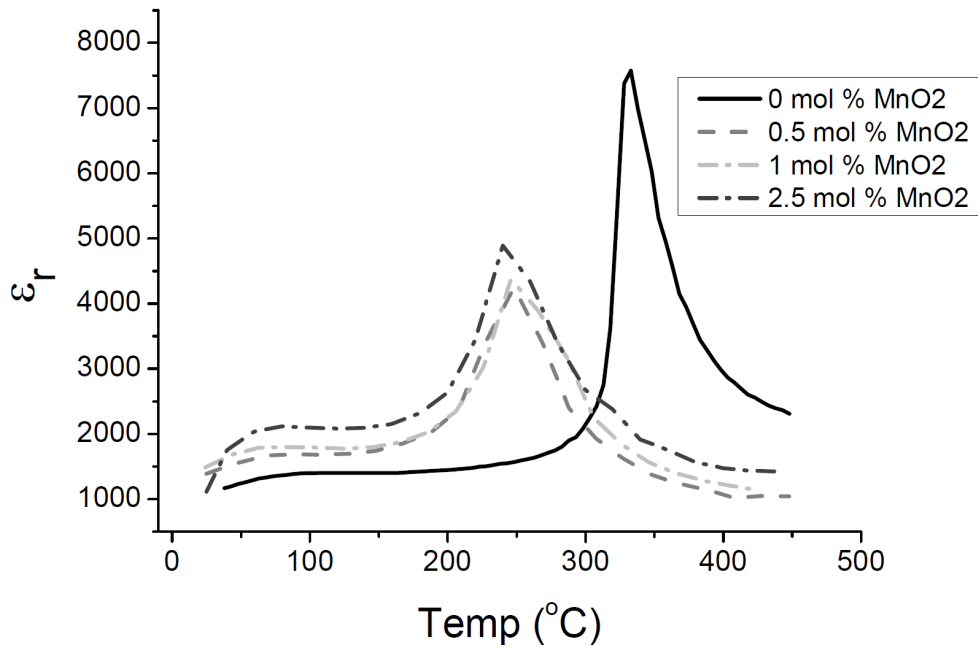


Fig 3a

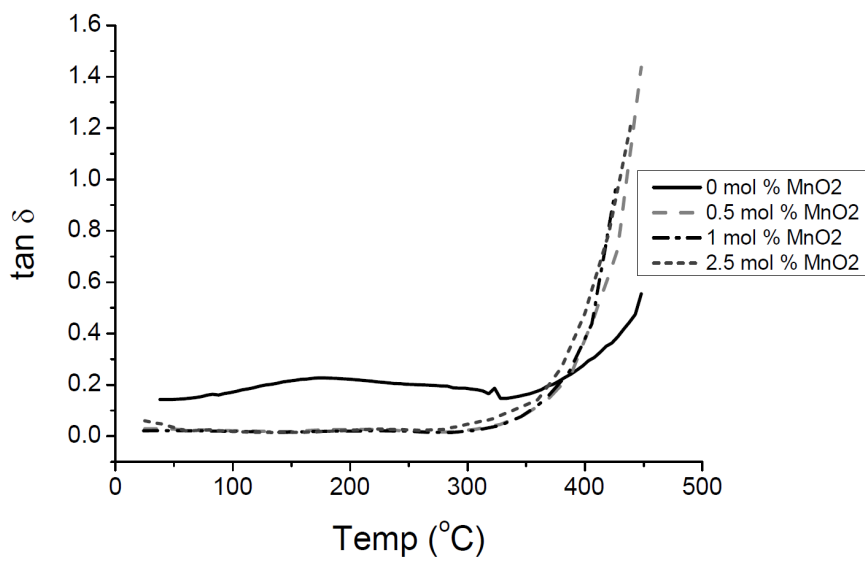


Fig. 3b

Fig. 3 High temperature dielectric constant (ϵ_r) and dielectric loss ($\tan \delta$) values for MnO_2 doped $\text{KNN-LiTaO}_3\text{-LiSbO}_3$ ceramics as a function of temperature.

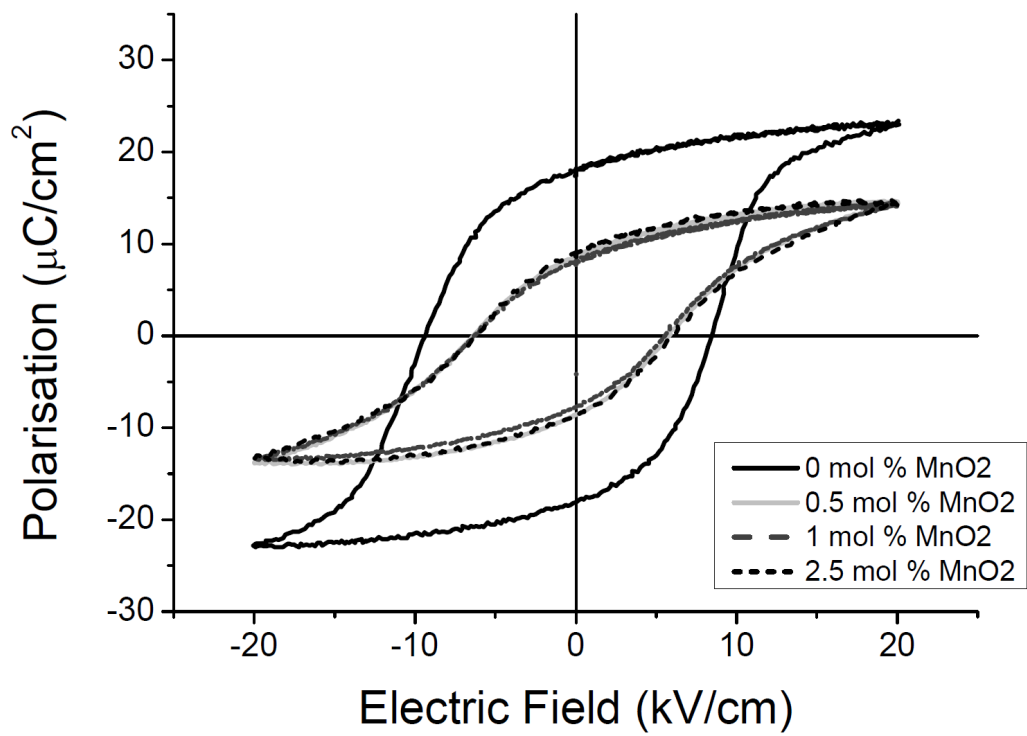


Fig. 4

Fig. 4 Variation of P-E hysteresis loops for MnO_2 doped $\text{KNN-LiTaO}_3\text{-LiSbO}_3$ ceramics.

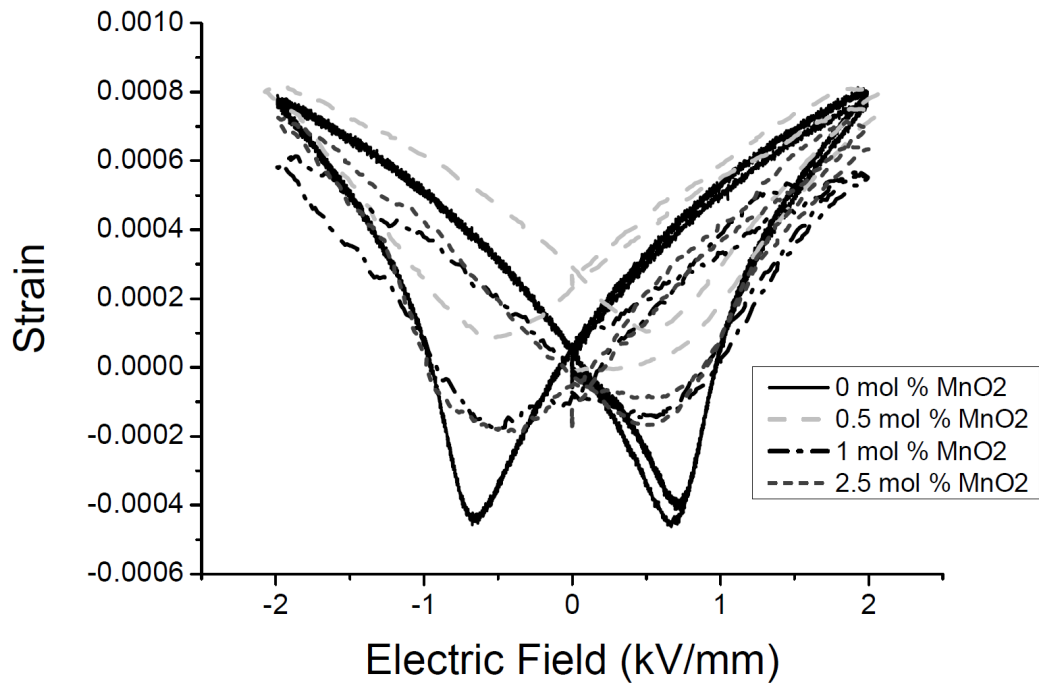


Fig. 5

Fig. 5 Variation of strain-field hysteresis loops for MnO₂ doped KNN-LiTaO₃-LiSbO₃ Ceramics

Table 1: Data showing the density, dielectric and piezoelectric properties of KNN-LiTaO₃-LiSbO₃ with different amounts of MnO₂ at room temperature.

Table 1

Composition	0 mol %	0.5 mol %	1 mol %	2.5 mol %
Theoretical density [g/cm ³]	4.79	4.8	4.81	4.83
Relative density [%]	94.3	95.7	96.4	94.4
Coercive field (E _c) [kV/mm]	8.6	5.6	5.8	6.2
Remanent Polarisation (P _r) [μC/cm ²]	18.3	8.6	8.3	8.9
Relative Permittivity(ε _r) @ 10kHz	1146	1387	1486	1117
Tan δ @ 10kHz	0.1515	0.0284	0.0215	0.0212
Piezoelectric constant (d ₃₃) [pm/V] (small signal)	220	171	171	176
Piezoelectric constant (d ₃₃)* [pm/V](large signal)	362.9	261.5	331.4	209.1

*The d₃₃ values from large signal measurements were obtained from the slope of the uniaxial strain hysteresis graphs.